



A quasi-three-dimensional numerical calculation procedure for periodically fully-developed heat and fluid flow

Numerical calculation procedure

379

A. Nakayama and F. Kuwahara

Department of Mechanical Engineering, Shizuoka University, Hamamatsu, Japan

Received July 2003
Revised February 2004
Accepted February 2004

Abstract

Purpose – To introduce a novel numerical calculation procedure for periodically fully developed heat and fluid flow, which can treat three-dimensional velocity and temperature fields, using a two-dimensional storage.

Design/methodology/approach – The three-dimensional Navier-Stokes equation and energy equation have been transformed into quasi-three-dimensional forms. An appropriate set of explicit periodic boundary conditions have been obtained for thermally fully developed flow through a general three-dimensional periodic structure, exploiting the volume averaging theory.

Findings – The proposed numerical procedure has been found inexpensive and efficient. Its validity has been proved by comparing the results obtained for a bank of long cylinders in yaw against available experimental data.

Originality/value – Since no explicit sets of periodic boundary conditions of this kind have been reported before, they will be exploited by researchers and practitioners interested in efficient numerical computations of three-dimensional periodic heat and fluid flows.

Keywords Flow measurement, Numerical analysis, Heat measurement

Paper type Research paper

Nomenclature

a_f	= specific interfacial area	k_f	= thermal conductivity
A_{int}	= total interface between the fluid and solid	$\vec{l}, \vec{m}, \vec{n}$	= Cartesian unit vectors
c_{p_f}	= specific heat capacity at constant pressure	Re_D	= Reynolds number based on D and the maximum velocity
D	= size of square rod	s	= coordinate along the macroscopic flow direction
Eu	= Euler number	V	= elementary representative volume
H, L, M	= size of structural unit	x, y, z	= Cartesian coordinates
h_f	= interfacial convective heat transfer coefficient	α, β, γ	= angles between the macroscopic velocity vector and principal axes
Pr_f	= Prandtl number	α'	= cross flow angle (projected angle)
u, v, w	= microscopic velocity components in the x, y and z directions	ν_f	= kinematic viscosity
T	= microscopic temperature	ρ_f	= density
p	= microscopic pressure	μ_f	= viscosity
		τ	= similarity factor



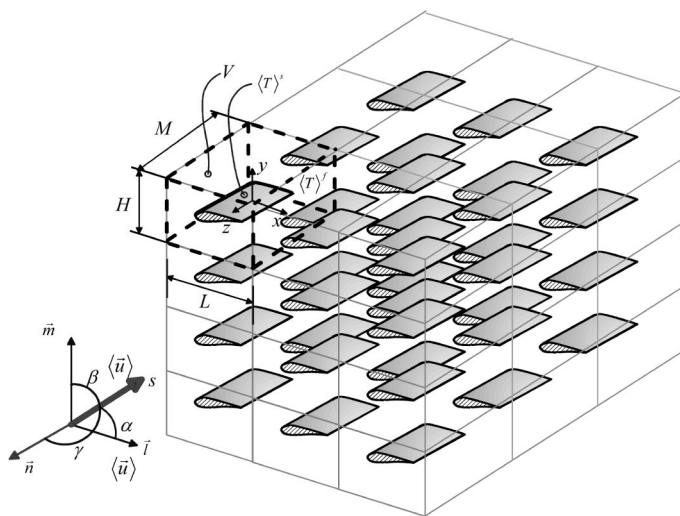
Introduction

In numerical computations, periodic boundary conditions are often used to obtain both velocity and temperature fields within manmade periodic structures, such as banks of tubes, arrays of fins, and conduits with periodically shaped wall surfaces. Patankar *et al.* (1977) prescribed the pressure drop over one structural unit to attack the problem of fully developed flow and heat transfer in ducts having streamwise-periodic variations of cross-sectional area, while Nakayama *et al.* (1995) and Kuwahara *et al.* (2001) chose to prescribe the mass flow rate (rather than the pressure drop) to obtain the fully developed velocity and temperature fields within two-dimensional periodic arrays.

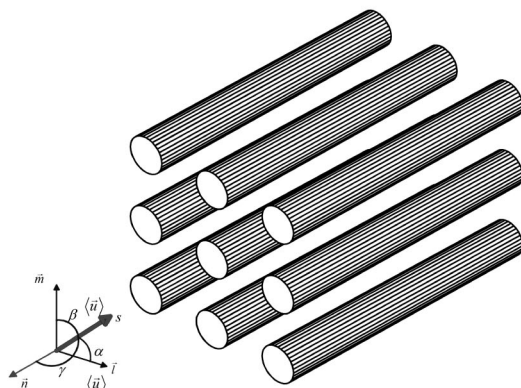
The prescription of the periodic boundary conditions for the velocity field (or pressure field) is rather straightforward, since the profiles at both upstream and downstream boundaries must be identical. However, that of the temperature field requires some consideration, when the surface wall temperature is kept constant. Naturally, the temperature difference between the fluid and solid wall becomes vanishingly small at the fully developed stage, as in the case of thermally fully developed tube flow with uniform surface temperature.

Our literature survey has revealed that no explicit thermal boundary conditions are available for analyzing three-dimensional flow and heat transfer within a three-dimensional periodic structure, such as shown in Figure 1(a). In this study, we shall obtain explicit thermal boundary conditions for the case of fully three-dimensional flow and heat transfer within a three-dimensional periodic structure with uniform surface temperature, appealing to the volume averaging theory, extensively used in the field of porous media (e.g. Cheng, 1978, Vafai and Tien, 1981, Quintard and Whitaker, 1993, Nakayama, 1995). Then, the three-dimensional heat and fluid flow through a two-dimensional periodic structure such as that through a bank of infinitely long cylinders in yaw, as shown in Figure 1(b), is considered. Especially for such three-dimensional heat and fluid flow, an economical quasi-three-dimensional calculation procedure is possible, so as to replace exhaustive full three-dimensional numerical manipulations. It will be shown that, under a macroscopically uniform flow through a two-dimensional structure, the three-dimensional governing equations reduce to quasi-three-dimensional forms, in which all derivatives associated with the axis of the cylinder can be either eliminated or replaced by other determinable expressions. Thus, only two-dimensional storages are required for the dependent variables in question. This substantially saves both CPU time and storage.

Some researchers, including Grimson (1937, 1938), Omohundro *et al.* (1949), Bergelin *et al.* (1950, 1952) and Zukauskas (1987), carried out extensive experimental investigations for heat transfer from a bundle of tubes in cross flow, and provided useful experimental data and correlations for designing cross-flow heat exchangers. However, these experimental data are limited to a certain class of geometrical



(a) Three-dimensional periodic structure



(b) Two-dimensional periodic structure

Figure 1.
Periodic structures

configurations such as tube banks for aligned and staggered arrangements, subject to a limited number of sets of transverse and longitudinal pitches. In particular, the data accounting for the yaw effects (i.e. the three-dimensional effects) are hardly available in the literature. In designing a particular heat exchanger, the correlations for the pressure drop and interfacial heat transfer coefficient, as functions of the macroscopic velocity vector (i.e. its magnitude and direction in reference to the axis of the tube) and other structural parameters, are definitely needed (Kays and London, 1984). The present quasi-three-dimensional numerical calculation procedure can be exploited to conduct a numerical experiment, so as to establish such hydrodynamic and thermal correlations for a given specific configuration.

Volume-averaging theory

We shall find an appropriate set of periodic boundary conditions for three-dimensional periodic structure, using the volume averaging theory. Let us assume a macroscopically uniform steady flow through a three-dimensional periodic structure of infinite extent as shown in Figure 1(a). The body shape of the structural element is arbitrary, and its arrangement can be aligned as in Figure 1(a) or staggered in an arbitrary fashion. Upon referring to the orthogonal unit vectors ($\vec{l}, \vec{m}, \vec{n}$) as shown in Figure 1(a), the macroscopically steady and uniform velocity field may be presented by

$$\langle \vec{u} \rangle = |\langle \vec{u} \rangle| (\cos \alpha \vec{l} + \cos \beta \vec{m} + \cos \gamma \vec{n}) \tag{1}$$

where

$$\langle \vec{u} \rangle = \int_V \vec{u} dV \tag{2}$$

is the volume averaged velocity vector averaged over a structural volume element V (i.e. Darcian vector, apparent velocity). The directional cosines of the volume averaged velocity satisfy the obvious relationship, namely,

$$\cos^2 \alpha + \cos^2 \beta + \cos^2 \gamma = 1 \tag{3}$$

This relation may be rewritten equivalently using the cross-flow angle α' projected onto the x - y plane as

$$\cos \alpha = \sin \gamma \cos \alpha' \text{ and } \cos \beta = \sin \gamma \sin \alpha' \tag{4}$$

We shall assume that the wall surfaces of the structure are maintained at a constant temperature. Then, the microscopic temperature field, when averaged spatially within a local structural control volume V , should lead to the macroscopic temperature field whose gradient aligns with the macroscopic velocity vector in the s direction, such that the volume averaged energy equation under the macroscopically steady and uniform velocity field with negligible macroscopic longitudinal conduction reduces to

$$\rho_f c_{p_f} |\langle \vec{u} \rangle| \frac{d\langle T \rangle^f}{ds} = -h_f a_f (\langle T \rangle^f - \langle T \rangle^s) \tag{5}$$

where

$$\langle T \rangle^{f,s} = \frac{1}{V_{f,s}} \int_{V_{f,s}} T dV \tag{6}$$

such that $\langle T \rangle^f$ and $\langle T \rangle^s$ denote the intrinsic averaged temperature of fluid and that of the structure, respectively. Note that V_f and V_s are the volumes of fluid and solid, respectively, within the structural elementary volume ($V = V_f + V_s$). Moreover, the interfacial heat transfer coefficient in the RHS of equation (5) is defined by

$$h_f \equiv \frac{\frac{1}{V} \int_{A_{int}} k_f \frac{\partial T}{\partial x_j} n_j dA}{(\langle T \rangle^s - \langle T \rangle^f)} \tag{7}$$

where n_i is the unit vector normal to the interface pointing from the fluid side to solid side. The net heat transfer between the fluid and solid is given by $h_f a_f (\langle T \rangle^f - \langle T \rangle^s)$ where a_f is the specific interfacial area (i.e. interfacial area per unit volume). Since the surface temperature of the structure $\langle T \rangle^s$ is constant, equation (5) naturally yields the macroscopic temperature field as

$$\langle T \rangle^f - (T)^s = (\langle T \rangle^f - (T)^s)_{\text{ref}} \exp\left(-\frac{a_f h_f}{\rho_f c_{p_f} |\langle \vec{u} \rangle|} (s - s_{\text{ref}})\right) \quad (8)$$

Note that the interfacial heat transfer coefficient h_f is expected to be constant for the periodically fully developed heat and fluid flow, as in the cases of thermally fully developed tube and channel flows. The correct set of the periodic boundary conditions in question should lead to the microscopic temperature field compatible with the macroscopic temperature field as given by equation (8). (In other words, the resulting microscopic temperature field, when averaged spatially, must yield the macroscopic temperature field given by equation (8).)

Periodic boundary conditions for three-dimensional periodic structure

In order to appreciate the foregoing argument based on the volume averaging theory, let us consider one of the simplest temperature fields, namely, the fully developed temperature field for the case of forced convection from isothermal parallel plates with a channel height H , as shown in Figure 2.

The thermally fully developed flow of this kind may be regarded as one of the special periodically fully developed flows, since the temperature profile at $x = x_0$ is *similar* to that at $x = x_0 + L$, such that

$$\frac{T(x_0 + L, y) - T_w}{T_B(x_0 + L) - T_w} = \frac{T(x_0, y) - T_w}{T_B(x_0) - T_w} \quad (9)$$

where L is any axial distance of arbitrary size (which may be unlimitedly large or small), and T_B is the bulk mean temperature. This can be rearranged as

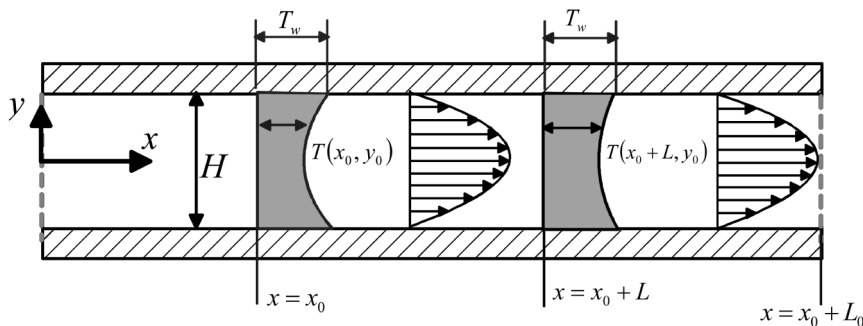


Figure 2.
Fully developed channel
flow

$$\frac{T(x_0 + L, y) - T_w}{T(x_0, y) - T_w} = \frac{T_B(x_0 + L) - T_w}{T_B(x_0) - T_w} = \exp\left(-\frac{2h_f L}{\rho_f c_{pf} u_B H}\right). \quad (10)$$

The last expression in the RHS comes from equation (8), as we note that $|\langle \vec{u} \rangle| = u_B$, $\langle T \rangle^f = T_B$, $\langle T \rangle^s = T_w$, and $a_f = 2/H$ for this case. Selecting a reference axial distance L_0 along an arbitrary level at $y = y_0$

$$\frac{T(x_0 + L_0, y_0) - T_w}{T(x_0, y_0) - T_w} = \exp\left(-\frac{2h_f L_0}{\rho_f c_{pf} u_B H}\right). \quad (11)$$

Upon combining equations (10) and (11), we obtain

$$T(x_0 + L, y) - T_w = (T(x_0, y) - T_w) \tau^{\frac{L}{L_0}} \quad (12)$$

where

$$\tau \equiv \frac{T(x_0 + L_0, y_0) - T_w}{T(x_0, y_0) - T_w}. \quad (13)$$

Hence, equation (12) is a possible expression for the thermally periodic boundary condition for this simple case, which guarantees us to yield the macroscopic temperature field compatible with equation (8). It is straightforward to extend the case to an infinite series of flat plates of finite length, to the two-dimensional periodic structure of arbitrary shape, and finally to a general three-dimensional periodic structure, as shown in Figure 1(a).

Thus, the steady-state governing equations and their correct set of the boundary conditions for periodically fully developed heat and fluid flow through a three-dimensional periodic structure are given as follows:

$$\nabla \cdot \vec{u} = 0 \quad (14)$$

$$\rho_f (\nabla \cdot \vec{u}) \vec{u} = -\nabla p + \mu_f \nabla^2 \vec{u} \quad (15)$$

$$\rho_f c_{pf} \nabla \cdot (\vec{u} T) = k_f \nabla^2 T. \quad (16)$$

On the solid walls:

$$\vec{u} = \vec{0} \quad (17a)$$

$$T = T_w (= \langle T \rangle^s). \quad (17b)$$

On the periodic boundaries:

$$\vec{u}|_{x=-\frac{L}{2}} = \vec{u}|_{x=\frac{L}{2}} \quad (18a)$$

$$\vec{u}|_{y=-\frac{H}{2}} = \vec{u}|_{y=\frac{H}{2}} \quad (18b)$$

$$\vec{u}|_{z=-\frac{M}{2}} = \vec{u}|_{z=\frac{M}{2}} \quad (18c)$$

where the origin of the Cartesian coordinates (x, y, z) is set in the center of the structural unit $(-L/2 \leq x \leq L/2, -H/2 \leq y \leq H/2, -M/2 \leq z \leq M/2)$, as indicated in Figure 1(a). The mass flow rate constraints are given by:

$$\int_{-\frac{M}{2}}^{\frac{M}{2}} \int_{-\frac{H}{2}}^{\frac{H}{2}} u \, dy \, dz \Big|_{x=-\frac{L}{2}} = \int_{-\frac{M}{2}}^{\frac{M}{2}} \int_{-\frac{H}{2}}^{\frac{H}{2}} u \, dy \, dz \Big|_{x=\frac{L}{2}} = HM \cos \alpha \langle |\vec{u}| \rangle \quad (19a)$$

$$\int_{-\frac{M}{2}}^{\frac{M}{2}} \int_{-\frac{L}{2}}^{\frac{L}{2}} v \, dx \, dz \Big|_{y=-\frac{H}{2}} = \int_{-\frac{M}{2}}^{\frac{M}{2}} \int_{-\frac{L}{2}}^{\frac{L}{2}} v \, dx \, dz \Big|_{y=\frac{H}{2}} = LM \cos \beta \langle |\vec{u}| \rangle \quad (19b)$$

$$\int_{-\frac{H}{2}}^{\frac{H}{2}} \int_{-\frac{L}{2}}^{\frac{L}{2}} w \, dx \, dy \Big|_{z=-\frac{M}{2}} = \int_{-\frac{H}{2}}^{\frac{H}{2}} \int_{-\frac{L}{2}}^{\frac{L}{2}} w \, dx \, dy \Big|_{z=\frac{M}{2}} = LH \cos \gamma \langle |\vec{u}| \rangle. \quad (19c)$$

Finally, the thermal boundary conditions for the periodic boundaries are given by

$$(T - T_w)|_{x=\frac{L}{2}} = \tau \frac{L \cos \alpha}{L \cos \alpha + H \cos \beta + M \cos \gamma} (T - T_w)|_{x=-\frac{L}{2}} \quad (20a)$$

$$(T - T_w)|_{y=\frac{H}{2}} = \tau \frac{H \cos \beta}{L \cos \alpha + H \cos \beta + M \cos \gamma} (T - T_w)|_{y=-\frac{H}{2}} \quad (20b)$$

$$(T - T_w)|_{z=\frac{M}{2}} = \tau \frac{M \cos \gamma}{L \cos \alpha + H \cos \beta + M \cos \gamma} (T - T_w)|_{z=-\frac{M}{2}} \quad (20c)$$

where

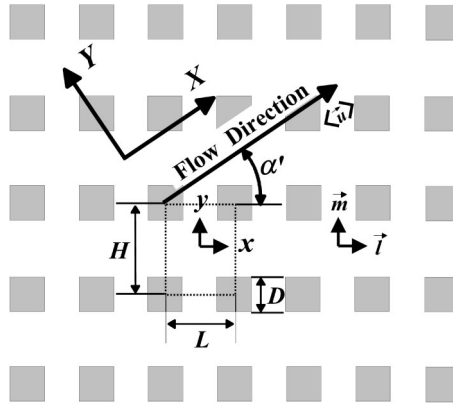
$$\tau = \frac{(T - T_w)|_{x=\frac{L}{2}, y=\frac{H}{2}, z=\frac{M}{2}}}{(T - T_w)|_{x=-\frac{L}{2}, y=-\frac{H}{2}, z=-\frac{M}{2}}}. \quad (21)$$

Our literature survey has revealed that no explicit periodic thermal boundary conditions (such as given by equations (20a)-(20c)) have been reported for three-dimensional periodic heat and fluid flows of this kind.

Quasi-three-dimensional numerical calculation procedure

The foregoing set of governing equations and corresponding boundary conditions may greatly be simplified for the case of the three-dimensional heat and fluid flow through a two-dimensional periodic structure such as a bank of cylinders in yaw, as illustrated in Figure 1(b) and more specifically in Figure 3 to show the cross-sectional plane of the square cylinder bank. All square cylinders in the figure, which may be regarded as heat sinks (or sources), are maintained at a constant temperature $T_w (= \langle T \rangle^s)$, which is lower (or higher) than the temperature of the flowing fluid. Since the cylinders are infinitely long, the set of the governing equations reduces to a quasi-three-dimensional form, in consideration of the limiting case, namely, $M \rightarrow 0$:

Figure 3.
Bank of square cylinders
(cross-sectional view)



$$\frac{\partial u}{\partial x} + \frac{\partial v}{\partial y} = 0 \tag{22}$$

$$\frac{\partial}{\partial x} \left(u^2 - \nu \frac{\partial u}{\partial x} \right) + \frac{\partial}{\partial y} \left(uv - \nu \frac{\partial u}{\partial y} \right) = -\frac{1}{\rho} \frac{\partial p}{\partial x} \tag{23}$$

$$\frac{\partial}{\partial x} \left(uv - \nu \frac{\partial v}{\partial x} \right) + \frac{\partial}{\partial y} \left(v^2 - \nu \frac{\partial v}{\partial y} \right) = -\frac{1}{\rho} \frac{\partial p}{\partial y} \tag{24}$$

$$\frac{\partial}{\partial x} \left(uw - \nu \frac{\partial w}{\partial x} \right) + \frac{\partial}{\partial y} \left(vw - \nu \frac{\partial w}{\partial y} \right) = \frac{\nu}{A_{\text{fluid}}} \oint_{P_{\text{int}}} \frac{\partial w}{\partial n} dP \tag{25}$$

$$\frac{\partial}{\partial x} \left(uT - \frac{\nu}{\text{Pr}_f} \frac{\partial T}{\partial x} \right) + \frac{\partial}{\partial y} \left(vT - \frac{\nu}{\text{Pr}_f} \frac{\partial T}{\partial y} \right) = S_w \tag{26}$$

where P is the coordinate along the wetted periphery whereas n is the coordinate normal to P pointing inward from the peripheral wall to fluid side. A_{fluid} is the passage area of the fluid, and

$$\begin{aligned} S_w &= -\frac{\partial}{\partial z} \left(wT - \frac{\nu}{\text{Pr}_f} \frac{\partial T}{\partial z} \right) \\ &= -\left(w - \frac{\nu}{\text{Pr}_f} \frac{\cos \gamma \ln \tau_0}{L \cos \alpha + H \cos \beta} \right) \frac{\cos \gamma \ln \tau_0}{L \cos \alpha + H \cos \beta} (T - T_w)|_{z=0} \end{aligned} \tag{27}$$

since

$$\frac{\partial T}{\partial z} = (T - T_w)|_{z=0} \lim_{M \rightarrow 0} \frac{\tau \frac{M \cos \gamma}{L \cos \alpha + H \cos \beta + M \cos \gamma} - 1}{M} = \frac{(T(x, y, 0) - T_w) \cos \gamma}{L \cos \alpha + H \cos \beta} \ln \tau_0 \quad (28)$$

where

$$\tau_0 \equiv \tau|_{z=0} = \frac{(T - T_w)|_{x=\frac{l}{2}, y=\frac{H}{2}, z=0}}{(T - T_w)|_{x=-\frac{l}{2}, y=-\frac{H}{2}, z=0}}. \quad (29)$$

The boundary and compatibility conditions for the periodic planes are given by

$$u|_{x=-\frac{l}{2}} = u|_{x=\frac{l}{2}} \quad (30a)$$

$$v|_{y=-\frac{H}{2}} = v|_{y=\frac{H}{2}} \quad (30b)$$

$$w|_{y=-\frac{H}{2}} = w|_{y=\frac{H}{2}} \quad (30c)$$

$$\int_{-\frac{H}{2}}^{\frac{H}{2}} u \, dy \Big|_{x=-\frac{l}{2}} = \int_{-\frac{H}{2}}^{\frac{H}{2}} u \, dy \Big|_{x=\frac{l}{2}} = H \cos \alpha \langle |\vec{u}| \rangle \quad (31a)$$

$$\int_{-\frac{l}{2}}^{\frac{l}{2}} v \, dx \Big|_{y=-\frac{H}{2}} = \int_{-\frac{l}{2}}^{\frac{l}{2}} v \, dx \Big|_{y=\frac{H}{2}} = L \cos \beta \langle |\vec{v}| \rangle \quad (31b)$$

$$\int_{-\frac{H}{2}}^{\frac{H}{2}} \int_{-\frac{l}{2}}^{\frac{l}{2}} w \, dx \, dy = LH \cos \gamma \langle |\vec{w}| \rangle \quad (31c)$$

$$(T - T_w)|_{x=\frac{l}{2}} = \tau_0^{\frac{L \cos \alpha}{L \cos \alpha + H \cos \beta}} (T - T_w)|_{x=-\frac{l}{2}} \quad (32a)$$

$$(T - T_w)|_{y=\frac{H}{2}} = \tau_0^{\frac{H \cos \beta}{L \cos \alpha + H \cos \beta}} (T - T_w)|_{y=-\frac{H}{2}} \quad (32b)$$

In this way, all derivatives associated with z can be eliminated. Thus, only two-dimensional storages are required to solve equations (22)-(26). (Note that both equations (25) and (26) may be treated as two-dimensional scalar transport equation.)

Method of computation and preliminary numerical consideration

The governing equations (22)-(24) subject to the foregoing boundary and compatibility conditions (30a), (30b), (31a), and (31b) were numerically solved using SIMPLE algorithm proposed by Patankar and Spalding (1972). As the u and v velocity fields were established, the remaining equations (25) and (26) subject to the boundary conditions (30c), (31c), (32a), and (32b) were solved to find w and T . Convergence was measured in terms of the maximum change in each variable during an iteration. The maximum change allowed for the convergence check was set to 10^{-5} , as the variables

are normalized by appropriate references. The hybrid scheme has been adopted for the advection terms. Further details on this numerical procedure can be found in Patankar (1980) and Nakayama *et al.* (1983). For the cases of square cylinder banks, all computations have been carried out for a one-structural unit $L \times H$ using non-uniform grid arrangements with 91×91 , after comparing the results against those obtained with 181×181 for some selected cases, and confirming that the results are independent of the grid system. All computations were performed using the computer system at Shizuoka University Computer Center.

In order to confirm the validity of the present numerical procedure based on the periodic boundary conditions, preliminary computations were also conducted for the case of forced convection from isothermal parallel plates with a channel height H , as shown in Figure 2. Since $\alpha = 0$, $\beta = \gamma = \pi/2$ for this case, we find $w = S_w = 0$, and

$$Nu_{2H} = \frac{h_f(2H)}{k_f} = \frac{\rho c_p u_B H^2}{L} \ln\left(\frac{1}{\tau_0}\right) \quad (33)$$

from equations (11) and (32a). The computations were made for $10 \leq Re_{2H} \leq 10^3$ and $Pr = 1$, and the numerical results for Nu_{2H} are presented in Figure 4. As increasing the Reynolds number, the Nusselt number attains its asymptotic value $Nu_{2H} \rightarrow 7.54$, which coincides with the exact solution.

Illustrative calculations for three-dimensional heat and fluid flow through a bank of cylinders in yaw

Validation of quasi-three-dimensional calculation procedure

The efficiency and accuracy of the quasi-three-dimensional calculation procedure, proposed for the two-dimensional structure, may be examined by comparing the results based on the procedure with those based on the full three-dimensional calculation procedure.

Extensive calculations have been carried out using the full three-dimensional governing equations (14)-(16) for macroscopically uniform flow through a bank of square cylinders in yaw, as illustrated in Figure 3. For this periodic structure, only the structural elementary volume $V = L \times H$, as indicated by dashed lines in the figure, may be taken as a calculation domain. The ratio H/L is set to 1, whereas the ratio D/H

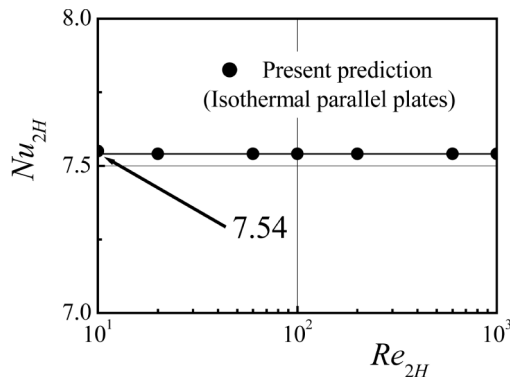


Figure 4.
Fully developed Nusselt number in a channel

is fixed to 1/2 for all calculations. The Reynolds number for the flow through a bank is usually defined by

$$Re_D = \frac{u_{\max} D}{\nu_f} = \frac{2|\langle \vec{u} \rangle| D}{\nu_f} \quad (34)$$

where the size of the cylinder D and the maximum velocity through the structure, $u_{\max} = |\langle \vec{u} \rangle| H / (H - D)$, are used as references.

In Figure 5, the resulting velocity and temperature fields obtained for the case of $H/L = 1$, $\alpha' = 45^\circ$, $\gamma = 45^\circ$, $Re_D = 600$ and $Pr_f = 1$ using the full three-dimensional calculation procedure (Figure 5(a)) are compared with those based on the quasi-three-dimensional calculation procedure based on the simplified governing equations (22)-(26) (Figure 5(b)). Excellent agreement between the two sets of the results can be seen, which verifies the accuracy and efficiency of the proposed quasi-three-dimensional calculation procedure. Moreover, the velocity and temperature profiles are plotted along some selected lines. These plots, which are not shown here, have proven that the difference between the two sets of the results is indiscernible. The CPU time required for the convergence using the full three-dimensional calculation turned out to be roughly 3h, six times more than that using the

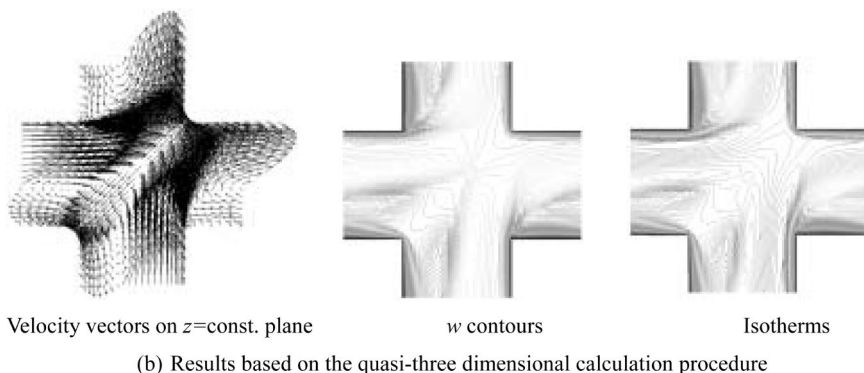
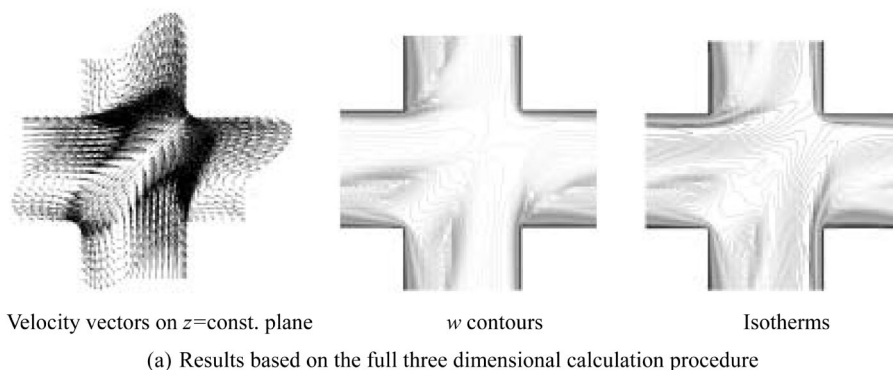


Figure 5.
Comparison of two
distinct three-dimensional
calculation procedures
($H/L = 1$, $\alpha' = 45^\circ$
 $\gamma = 45^\circ$, $Re_D = 600$,
 $Pr_f = 1$)

quasi-three-dimensional calculation. This proves the effectiveness of the quasi-three-dimensional calculation procedure.

This economical quasi-three-dimensional calculation procedure has been used to conduct a numerical experiment for macroscopically uniform flow through a bank of square cylinders in yaw over a wide range of the Reynolds number and flow angle.

Effect of cross-flow angle on Euler and Nusselt numbers

As we consider the effect of the cross flow angle α' , we shall fix the value of the yaw angle to $\gamma = \pi/2$, such that $\alpha' = \alpha$. Zukauskas (1982) assembled the experimental data for the fully developed pressure drop across the tube and presented a chart for the Euler number, which is defined by

$$Eu = \frac{2\Delta p}{\rho_f u_{\max}^2} \tag{35}$$

where Δp is the pressure drop per tube row. His inline-square arrangement (despite the difference in the cross-sectional shape) corresponds to the present arrangement with $\alpha = 0$, $\gamma = \pi/2$, and $H/D = 2$. It is also noted that, in reality, the macroscopic flow direction rarely coincides with the principal axes, since even small disturbances at a sufficiently high Reynolds number make the flow deviate from the axis. Thus, it is understood that the chart provided by Zukauskas gives only the average level of the pressure drop within a range of small α (say $0^\circ < \alpha < 5^\circ$). The Euler number obtained by Zukauskas from his pressure drop measurement for the case of $\gamma = \pi/2$ and $H/D = 2$ is plotted against Re_D in Figure 6, where the numerical results from our numerical experiment based on the quasi-three-dimensional calculation procedure are drawn together for three cross flow angles, namely, $\alpha = 0^\circ$, 5° , and 45° , so as to show the effect of cross-flow angle α on the Euler number. The predicted curve obtained at $\alpha = 5^\circ$ follows closely along Zukauskas' experimental curve.

The microscopic temperature results have been processed using equation (7) to obtain the interfacial heat transfer coefficient h_f . In Figure 7, the heat transfer results obtained at $\alpha = 0^\circ$, 5° , and 45° for the cross flows (i.e. $\gamma = \pi/2$) are presented in terms of the interfacial Nusselt number $Nu_D = h_f D/k_f$ against the Reynolds number Re_D . The figure suggests that the lower and higher Reynolds number data follow two distinct limiting lines for the cases of non-zero α . Unlike the Euler number, the

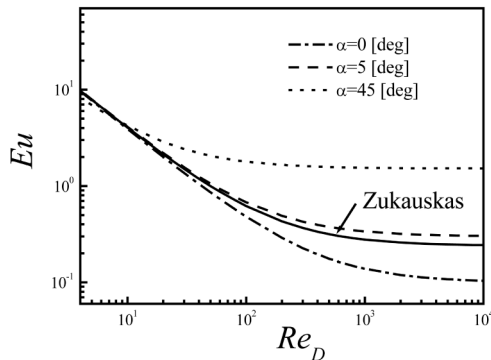


Figure 6.
Effect of Reynolds number
on Euler number

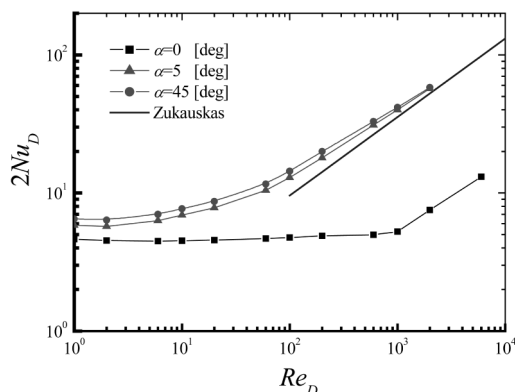


Figure 7.
Effect of Reynolds number
on interfacial Nusselt
number ($Pr = 1$)

interfacial Nusselt number is fairly insensitive to the (non-zero) cross-flow angle α . The lower Reynolds number data stay constant for the given array and flow angle, whereas the high Reynolds number data vary in proportion to $Re_D^{0.50.6}$. As already pointed out in connection with the pressure drop, it is quite unlikely to have the macroscopic flow align perfectly with the principal axes. Therefore, the curve predicted for $\alpha = 0$ should hardly be realized. The experimental correlation proposed by Zukauskas (1987) for the heat transfer from the circular tubes in staggered banks are compared with the present results obtained for the case of $\alpha = \pi/4$, $\gamma = \pi/2$, and $H/L = 1$. (Note $Nu_f \cong Nu_D$ and $Re_f \cong Re_D$ in equation (39) of Zukauskas since $H/D = 2$.) The present results follow closely along the experimental correlation of Zukauskas as increasing the Reynolds number.

Effect of yaw angle on Euler and Nusselt numbers

The pressure drop naturally decreases with decreasing the yaw angle γ from $\pi/2$. The correction factor, namely, the ratio of the Euler number $Eu(\gamma)/Eu(\pi/2)$ is often introduced for engineering use with the cross-flow angle α' being fixed. It should be noted that the ratio becomes insensitive to Re_D as increasing Re_D . The curve of the ratio of the Euler number generated by changing the yaw angle γ for the case of $\alpha' = 5^\circ$ is compared against that obtained from the experiment by Zukauskas (1982) in Figure 8, in which a good agreement can be seen. (Note that Zukauskas' in-line arrangement may correspond to the case of $\alpha' = 5^\circ$, as we judge from Figure 6.)

Zukauskas (1982) investigated the effect of the yaw angle on the interfacial heat transfer rate. He varied the yaw angle γ for both staggered and aligned arrangements, and compared the corresponding heat transfer rates for the same Reynolds number. He pointed out that the data when normalized by the value obtained at $\gamma = \pi/2$ for all staggered and inline arrangements, namely, $Nu_D(\gamma)/Nu_D(\pi/2)$, can be approximated by a single curve irrespective of the Reynolds number. His data for both staggered and inline arrangements are plotted together with our prediction in Figure 9. As in the case of the Euler number ratio, the Nusselt number ratio becomes insensitive to Re_D as increasing Re_D , and may be expressed as function of γ alone. The agreement between the experimental data and the prediction is fairly good, which again indicates the validity of our quasi-three-dimensional calculation procedure. (We are grateful to one of the reviewers who pointed out that the curve in Figure 9 is correlated well by

Figure 8.
Effect of yaw angle on Euler number

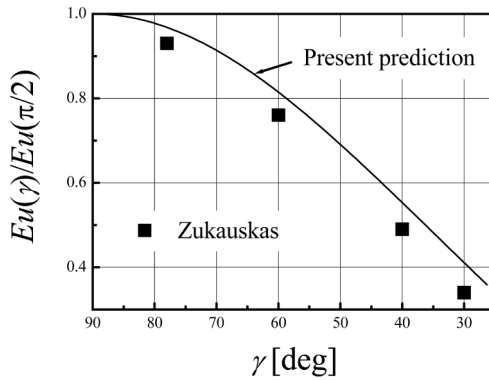
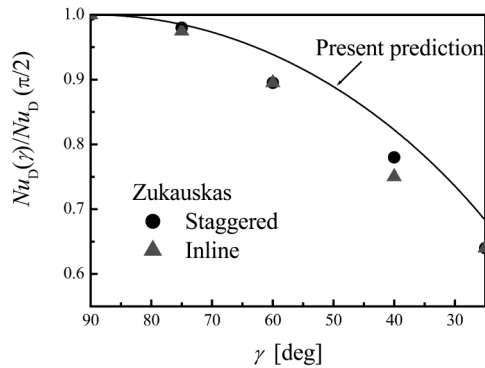


Figure 9.
Effect of yaw angle on interfacial Nusselt number



$Nu_D(\gamma)/Nu_D(\pi/2) = \sqrt{\sin \gamma}$, obtainable from the assumption that the Nusselt number is proportional to the square root of the Reynolds number based on the effective velocity $|\langle \vec{u} \rangle| \sin \gamma$.

Concluding remarks

An inexpensive and yet efficient numerical calculation procedure has been proposed for three-dimensional heat and fluid flow through a two-dimensional periodic structure in yaw. Explicit boundary conditions for the thermally fully developed periodic flow were obtained exploiting the volume averaging theory. The efficiency and accuracy of the proposed quasi-three-dimensional calculation procedure were examined by comparing the results based on the procedure with those based on the full three-dimensional calculation procedure. The CPU time required for the convergence using the quasi-three-dimensional computation turned out to be only one sixth of that for the full three-dimensional calculation computation, proving the effectiveness of the quasi-three-dimensional calculation procedure.

Extensive calculations have been carried out using this quasi-three-dimensional calculation procedure for macroscopically steady and uniform flow through a bank of square cylinders in yaw. The comparison of the numerical results with available experimental data has proven the validity of the present numerical procedure. The present quasi-three-dimensional numerical calculation procedure may be exploited

to conduct a numerical experiment for various heat transfer equipment, so as to establish possible hydrodynamic and thermal correlations for a given specific configuration.

References

- Bergelin, O.P., Brown, G.A. and Doberstein, S.C. (1952), "Heat transfer and fluid friction during viscous flow across banks of tubes – IV. A study of the transition zone between viscous and turbulent flow", *Transaction of ASME*, Vol. 74, pp. 953-60.
- Bergelin, O.P., Brown, G.A., Hull, H.L. and Sullivan, F.W. (1950), "Heat transfer and fluid friction during viscous flow across banks of tubes – III. A study of tube spacing and tube size", *Transaction of ASME*, Vol. 72, pp. 881-8.
- Cheng, P. (1978), "Heat transfer in geothermal systems", *Advances in Heat Transfer*, Vol. 14, pp. 1-105.
- Grimson, E.D. (1937), "Correlation and utilization of new data on flow resistance and heat transfer for cross flow of gases over tube banks", *Transaction of ASME*, Vol. 59, pp. 583-94.
- Grimson, E.D. (1938), "Heat transfer and flow resistance of gases over tube banks", *Transaction of ASME*, Vol. 58, pp. 381-92.
- Kays, W.M. and London, A.L. (1984), *Compact Heat Exchangers*, 3rd ed., McGraw-Hill, New York, NY.
- Kuwahara, F., Shirota, M. and Nakayama, A. (2001), "A numerical study of interfacial convective heat transfer coefficient in two-energy equation model for convection in porous media", *International Journal of Heat Mass Transfer*, Vol. 44, pp. 1153-9.
- Nakayama, A. (1995), *PC-Aided Numerical Heat Transfer and Convective Flow*, CRC Press, Boca Raton, FL.
- Nakayama, A., Chow, W.L. and Sharma, D. (1983), "Calculation of fully developed turbulent flows of ducts of arbitrary cross-section", *Journal of Fluid Mechanics*, Vol. 128, pp. 199-217.
- Nakayama, A., Kuwahara, F., Kawamura, Y. and Koyama, H. (1995), "Three-dimensional numerical simulation of flow through a microscopic porous structure", *Proc. ASME/JSME Thermal Engineering Conference*, Vol. 3, pp. 313-8.
- Omohundro, G.A., Bergelin, O.P. and Colburn, A.P. (1949), "Heat transfer and fluid friction during viscous flow across banks of tubes", *Transaction of ASME*, Vol. 71, pp. 583-94.
- Patankar, S.V. (1980), *Numerical Heat Transfer and Fluid Flow*, Hemisphere, Washington, DC.
- Patankar, S.V. and Spalding, D.B. (1972), "A calculation procedure for heat, mass and momentum transfer in three-dimensional parabolic flows", *International Journal of Heat Mass Transfer*, Vol. 15, pp. 1787-806.
- Patankar, S.V., Liu, C.H. and Sparrow, E.M. (1977), "Fully developed flow and heat transfer in ducts having streamwise-periodic variations of cross-sectional area", *Journal of Heat Transfer*, Vol. 99, pp. 180-6.
- Quintard, M. and Whitaker, S. (1993), "One and two equation models for transient diffusion in two-phase systems", *Advances in Heat Transfer*, Vol. 23, pp. 269-464.
- Vafai, K. and Tien, C.L. (1981), "Boundary and inertia effects on flow and heat transfer in porous media", *International Journal Heat Mass Transfer*, Vol. 24, pp. 195-203.
- Zukauskas, A. (1982), *Konvektivnyi Perenos v Teploobmennikakh (Convective Transfer in Heat Exchangers)*, Nauka, Moscow, p. 472.
- Zukauskas, A. (1987), "Heat transfer from tubes in crossflow", *Advances in Heat Transfer*, Vol. 18, pp. 87-159.